Journal of Materials Chemistry C

Accepted Manuscript

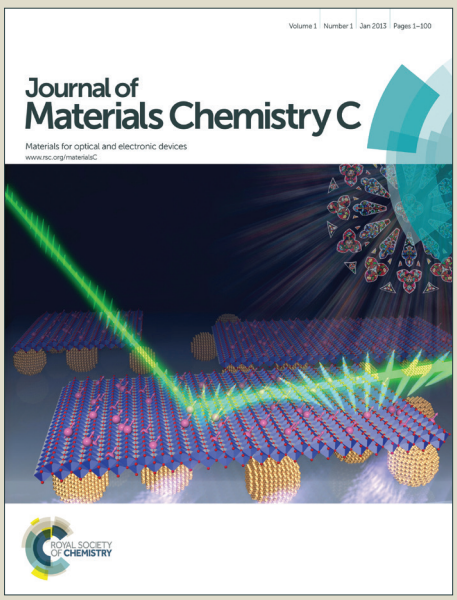

ROYAL SOCIETY OF CHEMISTRY

www.rsc.org/materialsC

Journal of Materials Chemistry C

ARTICLE

Synthesis of FeCo Alloy Magnetically-Aligned Linear Chains by Polyol Process: Structural and Magnetic Characterization

Received 00th January 20xx,
Accepted 00th January 20xx

DOI: 10.1039/x0xx00000x

www.rsc.org/

Dustin M. Clifford,[a] Carlos. E. Castano,[a] Amos J. Lu,[a] and Everett E. Carpenter [a]

FeCo alloy magnetically aligned linear chains (MALCs) were synthesized by the polyol process using a unique reaction format departing from conventional bench-top reactions. FeCo MALC morphology was obtained in the presence of an external dynamic magnetic field. XRD analysis confirmed body-centered cubic (bcc) FeCo alloy. Transverse and tangential to incident X-ray path XRD analyses of as-synthesized FeCo MALCs were performed further substantiating the linear chain morphology. Average chain diameter was at ≈ 206 ± 52 nm while Scherrer analysis of (110) gave an average crystallite size of 29 nm. Chemical attachment of each aligned FeCo alloy segment was confirmed by tangential cross-sectioning by focused ion beam (FIB). Electron diffraction confirmed the bcc FeCo phase with d-spacings of (110), (200) and (211) in good agreement from XRD. The as-synthesized FeCo alloy MALCs possessed a saturation magnetization value, M_s, of 205 emu/g and a coercivity, H_c, of 150 Oe at 300 K. Magnetization was recorded from 300 to 1000 K with increase at temperatures correlating to transitions from hcp Co/α^1 to fcc Co/α^1 at 500 K and to α^1 at 600 K for Co rich portions of the MALCs ($Fe_{32}Co_{68}$). Annealed (1000 K) FeCo MALCs possessed an M_s of 212 emu/g with H_c of 120 Oe. Morphological changes of the 1000 K annealed sample were microwire formation and secondary phase of cubic FeO. As-synthesized FeCo alloy MALCs as highly magnetic, air stable, non-tethered and high aspect ratio structures are candidates for radar absorbent materials (RAMs) when magnetically oriented in coatings or for magnetic sensing devices.

Introduction

FeCo alloys possess high permeability (μ), high saturation magnetization (M_s), high Curie temperature (T_C) and low coercivity (H_c). These remarkable properties of FeCo alloys allow for unique and diverse applications anywhere from magnetic recording read/write heads to magnetic sensing and electric motors or generators.[1] FeCo alloys (35 % *at.* Co) possess the highest M_s of any magnetic materials known and Co is the only element that increases M_s when alloyed with Fe.[2] FeCo alloy nanoparticles, depending on the atomic composition, may attain moment (bohr magneton) values greater than 2.4 μ_B, making them useful as magnetic resonance (MR) probes.[3] Therefore, investigating magnetic properties of FeCo alloys, specifically at nanoscopic and mesoscopic dimensions, is of current interest. When high aspect ratios (10-20) are achieved as in the case of Ni nanowires (NWs) or nanopillars, a decrease in T_C (Curie point) has been observed at diameters below 90 nm.[4] Nanoscale ferromagnetic materials such as Co NW arrays have shown an increase in H_c up to 4.8 kOe when the applied magnetic field was along the easy axis of the hcp-Co.[5] In contrast, low H_c values are routinely achieved in ferromagnetic alloys of FeCo due to larger dimensions and or annealing treatments that reduce internal strain and defects within the microstructure.[2]

FeCo alloy nanowire (NW) syntheses have been reported and they often involve complicated template assisted growth steps. Single crystal FeCo nanowires have been grown by thermolysis in carbon nanotubes (CNTs) where the CNT acted as the template but they are not stable and cannot be manipulated without CNT shells due to protection they provide against oxidation.[6] FeCo NW arrays grown using anodic aluminum oxide (AAO) resulted in H_c up to 2.8 kOe when the applied field was parallel to the FeCo NW arrays after annealing at 500 C for 2 hrs.[1] Other synthetic routes of high aspect ratio magnetic structures include thermal decomposition, physical vapor deposition (PVD) and solvothermal methods. Thermal decomposition has been

[a] *Virginia Commonwealth University, Richmond, VA 23284.*
† Footnotes relating to the title and/or authors should appear here.
Electronic Supplementary Information (ESI) available: EDS results, SEM of FeCo particles synthesized without external magnetic field, and zfc and fc cooling curves of as synthesized MALCs.See DOI: 10.1039/x0xx00000x

reported on synthesis of CoCr NWs, whereby decomposition of $Co_2(CO)_8/Cr(CO)_6$ occurred in the presence of a magnetic field.[7]

FeCo alloy magnetically aligned linear chains (MALCs) were synthesized for the first time using a specialized reaction formation under the polyol process. One major advantage of performing wet-chemical solvothermal routes, such as the polyol process used in this work, is that the materials are produced in a free powder form after cleaning. The polyol process involves the reduction of a metal salt precursor in a polyol (solvent) such as propylene glycol or ethylene glycol. Sodium hydroxide, an initiator, when added in sufficient concentration, facilitates glycolate anion formation by deprotonation of the glycol solvent, in which in itself, acts as a reducing agent of the metallic precursors. Reports on the polyol process to synthesize FeCo nanoparticles have been made in the 2010's.[8-11] These include size tuning of FeCo dice performed by adjusting the overall metal ion concentration from 0.07 to 0.015 mol/L, generating particle sizes ranging from 35 to 300 nm.[12] Furthermore, scaled-up preparations of FeCo nanoparticles have been performed using the polyol process demonstrating high moments.[13] However, to the authors' best knowledge, no FeCo alloy magnetically aligned linear chains (MALCs) syntheses have been reported using the polyol process.

The synthesis of FeCo MALCs was done so under a dynamic external magnetic field created by a permanent magnet mounted to a pneumatic piston. A representation of the reaction format is shown in Fig. 1. As the permanent magnet oscillates parallel (about 2.0 cm) from the reaction vessel, a PTFE coated permanent magnet within the reaction tube oscillates in unison creating vertical stirring for the reaction. The magnetic flux density of the external magnet was calculated to be approximately 0.24 T based on dimensions of the AlNiCo cylindrical magnet (*D=1.5 cm, L=3.5 cm*).

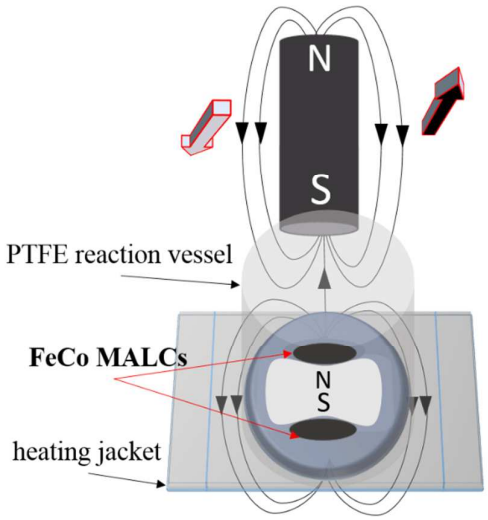

Fig. 1. Single reaction vessel representation of magnetically-controlled vertical stirring used to synthesize FeCo MALCs with general magnetic flux lines shown.

This unique reaction format, under proper reaction conditions and temperature ramp rates, facilitates non-classical growth of FeCo MALCs. A generalized mechanism for the formation of FeCo alloy MALCs begins with FeCo alloy particle growth first by reduction and subsequent nucleation of $Fe^{(0)}$ and $Co^{(0)}$ into crystalline FeCo alloy particles followed by spontaneous magnetic alignment and continued growth into linear structures. Intriguingly, in an absence of an external field during synthesis, no MALC morphology was observed, rather, a presence of FeCo alloy cubes and spheroids with similar diameters of the MALCs (see supplemental S1). This observation indicates the dominant role of the applied magnetic field in MALC formation. The as-synthesized FeCo MALCs have potential applications in coating technology where they may be employed as a radar-absorbent material (RAM) in avoiding hostile radar detection, though no such study has been performed here.[14]

Experimental

FeCo Alloy Precursor Solution Preparation. Iron (II) chloride tetrahydrate and cobalt (II) acetate tetrahydrate were massed and added to a (under N_2) round bottom flask containing ethylene glycol giving an overall $[Me^+]$ of 0.7 M and a molar ratio of [Fe] and [Co] 1.5 : 1. Gentle heating below 100 C was performed for 1 hr with magnetic stirring to ensure complete dissolution until a translucent fuchsia solution color was observed.

Synthesis of FeCo Alloy MALCs. For each reaction vessel, 25 mL of the precursor solution was transferred by volumetric pipette. A cylindrical PTFE vessel (1" diameter, 8" length) was equipped with a vertical movement magnetic stir bar and temperature controlled heating jacket with a K-type

thermocouple at the base. Dry NaOH pellets were added to give [OH] in the range of 5-7 M while under vertical stirring immediately following temperature ramp in the range of 8-13 C/min. The reaction vessel was sealed and purged with N_2 atmosphere during the course of the reaction. Total reaction time ranged from 13-25 minutes dependent on when the temperature reached maximum at 150 C as based on desired ramp rate. Condensation at the top of the inner vessel wall was carefully monitored and prevented from returning to the reaction mixture by use of absorbent material in combination with controlled and gentle stirring to prevent splashing of reaction mixture.

Characterization. Phase identification of the FeCo alloy MALCs was performed by X-ray diffraction (XRD) (Panalytical X'pert Pro) in a Bragg-Brentano configuration using a 0.5 ° fixed divergence slit, 1.0 ° anti-scatter slit and 10 mm mask on incident X-ray side. HTXRD was performed using an Anton-Parr 1200N oven equipped with a stage height control and nitrogen atmosphere. A low background Si wafer was used for the HTXRD analysis. Morphological characterization was performed by scanning electron microscope (SEM) on a Hitachi SU-70. Energy Dispersive Spectroscopy (EDS) (at 15 KeV) and focus ion beam (FIB) cross-sections were performed on a Zeiss Auriga SEM. Transmission electron microscopy (TEM) including basic imaging and diffraction analysis was performed on a Zeiss Libra 120 using a LaB_6 filament operating at 120 keV acceleration voltage. Hysteretic magnetic characterizations were performed using a Quantum Design VersaLab vibrating sample magnetometer (VSM) with a -3 to 3 T saturation field. The zfc and fc analyses were measured in a constant field of 500 Oe

Results

The as synthesized MALCs were characterized using XRD from 20-85 2θ with Cu $K_{\alpha 1}$ radiation (λ=0.154056 nm) to identify the phase composition as shown in Fig. 2.

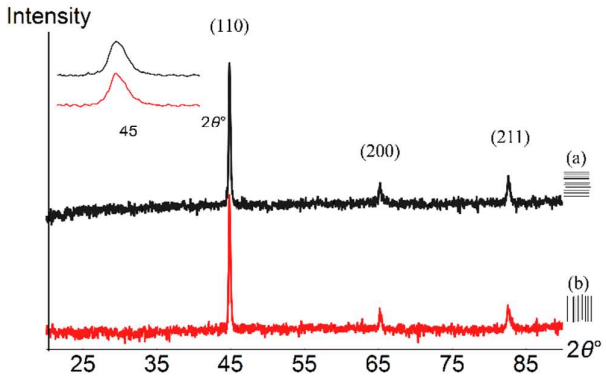

Fig. 2. XRD overlay showing bcc FeCo alloy from 20-85 2θ of two orientations, (a) parallel (top) and (b) perpendicular (bottom) to incident (overhead view) Cu K_{α} source and detector.

Bcc FeCo alloy was confirmed by comparison (pdf: 01-071-5029, $Fe_{50}Co_{50}$, a = 0.28570 nm) with the (110), (200) and (211) peaks shown in Fig. 2. Alignment of the FeCo MALCs was performed using a rare-earth magnet placed beneath a low background Si substrate and analyzed by XRD under two orientations of the MALCs respective to the overhead view of the incident X-ray path (see Fig. 2). The parallel orientation scan indicates a slightly higher intensity (<5%) (inset of Fig. 2) of the (110) plane since at lower angles the X-ray path travels through greater crystallite volume per MALC, while at higher angles, these diffraction intensities are shown to not differ significantly. Furthermore, both scans confirmed that the as-synthesized MALCs are isotropic and that no crystalline oxide phase impurities were present. Scherrer analysis from the (110) plane Fig. 2 (a) gives an estimate of the average crystallite size of ≈ 29 nm.

FeCo MALC morphology was studied under electron microscopy. SEM imaging was performed at 5.00 keV using electron back-scatter in combination with secondary electron detection as shown in Fig. 3. The MALC morphology is clearly represented as consisting of FeCo alloy quasi-cubic and spherical segments formed, constituting each MALC length. Average MALC diameter was approximately 206 ± 52 nm as determined from the chain diameter distribution (Fig. 3 (b)). This result is much higher that the Scherrer analysis result of 29 nm suggesting that each segment is polycrystalline.

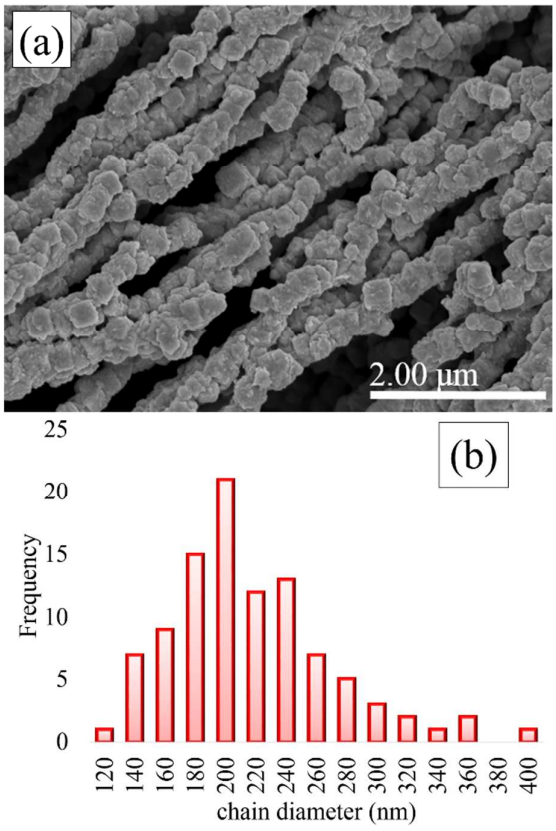

Fig. 3. SEM of FeCo MALCs (a) with chain diameter distribution (b) and average chain diameter $D_{(ave)}$ =206 ± 52 nm.

Elemental analysis was also performed using energy dispersive spectroscopy (EDS) at 15 keV (see supplemental S2) and averaged over six regions of the FeCo MALCs. The Fe:Co atomic ratio was calculated to be 58:42 respectively, indicating the complete reaction of Fe and Co precursors. Surface sensitive SEM imaging was not enough to confirm structural formation of the FeCo MALCs, therefore focused ion beam (FIB) was employed using Ga ions as a milling source by carefully cross-sectioning (tangentially) a magnetically oriented region of multi-stacked FeCo MALCs. FIB cross-sections of various FeCo MALCs from three separate regions of a single fixed lamella are shown in Fig. 4 (approx. thickness < 175 nm). As most of the MALCs were not agglomerated by a carbon passivation layer the structural stability of the MALC lamella was compromised. However, a few regions were located where carbon layer formation coated multiple MALCs, binding them together for further analysis.

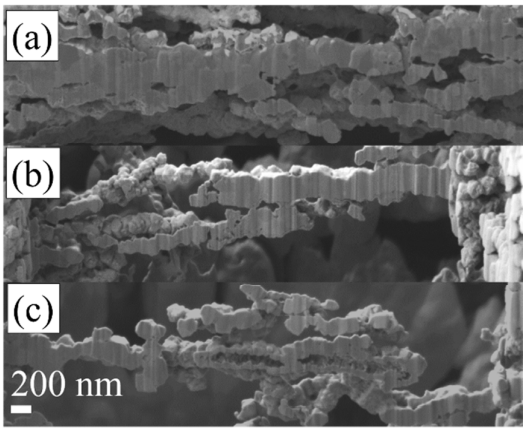

Fig. 4. Polished tangential cross-sections of stacked as-synthesized FeCo MALCs by focused ion beam (FIB) of three separate regions (a), (b) and (c) from the same milling plane indicating chemical attachment of FeCo cubic and spherical segments during growth of the MALCs.

Chemical attachment of the FeCo segments is likely the dominant structural formation process by several observations; observed structural continuity of the FeCo MALC in the tangential cross-section, different orientations of FeCo alloy segments where image contrast is observable by atomic density (lighter regions correspond to orientations showing increased phase density) in Fig. 4. (a) and the inherent structural rigidity of single FeCo MALCs as support (Fig. 4. (b) and (c)). Inadvertently a few transversal cross-sections of the FeCo MALCs were observed in Fig. 4 (c) as not all FeCo MALCs were in alignment during the tangential cross-sectioning process.

As-synthesized FeCo MALCs were annealed under vacuum with SEM images shown in Fig. 5. Sintering of the MALCs into larger diameter continuous microwires evolved within the 30 minute annealing period. In addition, evidence of a phase formation from the bcc phase of FeCo is indicated by the appearance of several crystallites on the surface of the large annealed FeCo microwires observable in Fig. 5 (b) (c) and (d). These structural changes were studied by quantitative point analysis using EDS indicating a non-stoichiometric cobalt ferrite phase formation (see supplemental S3) with an approximate atomic ratio of $CoFe_4O_{3.5}$ where point analysis by EDS from the main region of the FeCo alloy microwire indicate a $Fe_{47}Co_{53}$ atomic ratio (see supplemental S4). Based on these findings, it is clear that Fe became depleted from the original $Fe_{58}Co_{42}$ composition to form a secondary oxide phase on the surface during the annealing process.

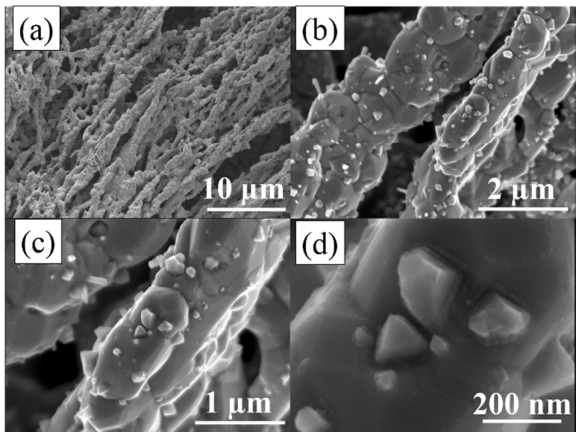

Fig. 5. FeCo MALCs annealed in vacuum at 1000 K for 30 minutes (a). Oxide phase formation indicated in (b), (c) and (d) due to crystallite formation on FeCo microwire surfaces.

To further probe this phase transition, the FeCo MALCs were analyzed by high temperature XRD (HTXRD) shown in Fig. 6 up to 1000 K (727 C). An observable phase transition starting at 600 C of cubic FeO was detected with enhancement of the phase at 1000 K (727 C). Upon cooling, the cubic FeO phase remained in the MALC sample and explains the observed crystallites formed in Fig. 5.

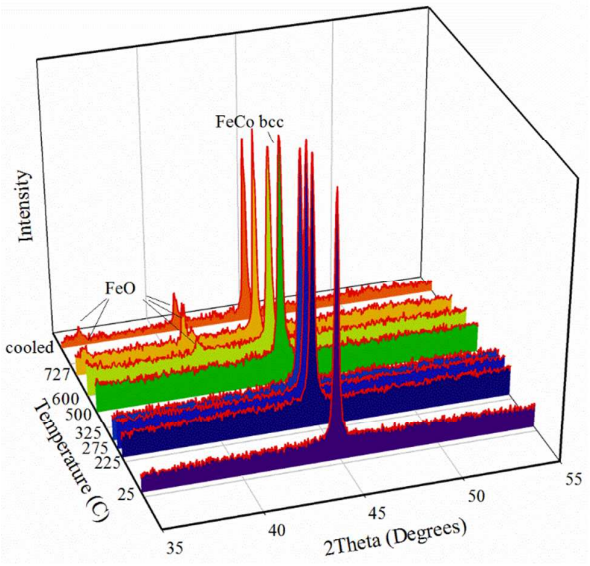

Fig. 6. HTXRD scans of FeCo MALCs annealed up to 727 C (1000 K) in N_2 and analyzed by HT-XRD at several temperatures.

In addition, a peak shift to lower 2θ of the FeCo bcc (110) peak was observed due to lattice expansion at higher temperatures. Slight splitting of the (110) peak of bcc FeCo at 1000 K was detected and can be attributed to the slight segregation of Co from the FeCo lattice from the B2 (ordered) to the A2 (disordered) phase transition.

A bright-field TEM image of two regions of as-synthesized FeCo MALCs was gathered shown in Fig. 7 (a). Individual segments are clearly seen comprising the length of the MALC structure. Selected area electron diffraction analysis (SAED) (Fig. 7 (b)) of the MALCs indicate the prominent FeCo bcc phase with the (211), (200) and (110) planes whose d-spacings agree with those from the XRD analysis (Fig. 2) as well as the XRD reference scan for a $Fe_{50}Co_{50}$ composition (pdf: 01-071-5029).

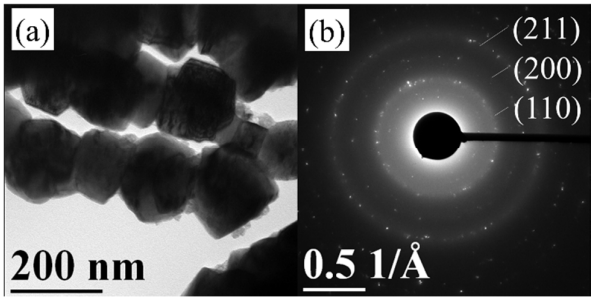

Fig. 7. TEM analysis of the as-synthesized FeCo MALCs (a) with SAED pattern (b) showing the bcc FeCo alloy (110), (200) and (211) Bragg reflections.

Hysteresis curves of the FeCo MALCs were measured in a sweeping external field from -3 to 3 T at 50, 300, 1000 and 300 K after anneal as shown in Fig. 8. The M_s, of the FeCo MALC sample at 300 K was measured to be 205 emu/g (SI units: $M_s \approx 1700 \times 10^3$ A/m, based on $\rho \approx 8.278$ g/cm^3 for $Fe_{60}Co_{40}$). At 1000 K, the M_s was 177 emu/g, a significantly lower value than that measured at 300 K, which can be explained by a partial transition from the ordered α^1 (B2) into the disordered (A2) α phase and loss of ferromagnetic order at elevated temperatures approaching the Curie temperature T_c. This order-disorder phase transition can be described as fcc Co crystallites forming by removal from the FeCo lattice thus contributing to the lower M_s value as has been shown in high temperature XRD studies.[15] As % Co in FeCo decreases, the moment (μ_B) may decrease up to 12 % according the Slater-Pauling curve for FeCo alloys.[16]

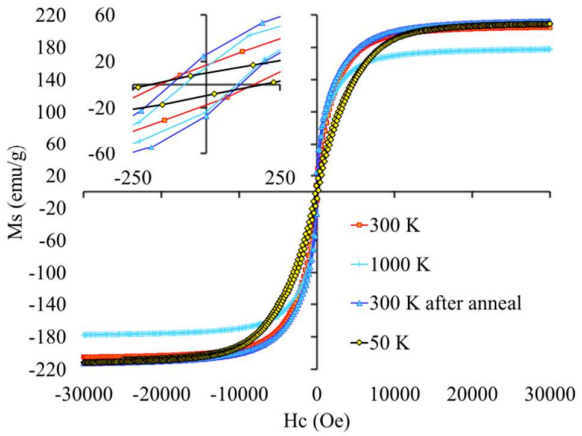

Fig. 8. Hysteretic curves of FeCo MALCs possessing saturation magnetization (Ms) of 209 (50 K), 205 (300 K), 177 (1000 K) and 212 (emu/g) (300 K after anneal).

The FeCo MALC sample was annealed at 1000 K for approximately 30 minutes using similar heating and cooling rates of 10 K/min. As mentioned above, for a $Fe_{60}Co_{40}$ composition at around 930 K, a transition from an ordered state to a disordered state where distribution of Fe and Co atoms decreases based on the FeCo phase diagram.[2] With the apparent formation of an FeO phase as shown in the HTXRD in Fig. 6 of the MALCs when annealed to 1000 K, a lower magnetization is expected, however, the annealed FeCo MALC sample possessed a slightly greater M_s of 212 emu/g which can be explained by the disorder to order transition of Fe and Co where ordering of both elements is promoted upon cooling. At this point, the diffusion of Co and Fe may redistribute more evenly into the lattice than before the sample was annealed. It is assumed that a decreased cool-down rate (ie. longer cool-down period) from 1000 K of the FeCo MALCs could result in higher moments, however, this study was not performed. The M_s of the FeCo MALCs (before anneal) increased slightly from 300 K at 50 K (209 emu/g) which can be explained by the least amount of thermal energy influence with the spin moments.

In order to further investigate the magnetic properties of the as-synthesized FeCo MALCs, zero-field (zfc) and field cooled (fc) curves (see supplemental S5) were acquired using the VSM under a field of 500 Oe of the as-synthesized FeCo MALCs. The fc curve, upper plot, indicates ferromagnetism of the FeCo MALCs since the zfc magnetization is lower than the fc curve in the 50-400 K temperature range shown. Similar studies on non-Fe containing Co nanoparticles also indicate a ferromagnetic response at these temperatures.[17]

Fig. 9 displays the mass susceptibility versus temperature (K) of the as-synthesized FeCo MALCs. The measurement was acquired using a VSM oven (in vacuum) containing a nanolithographic Pt/ceramic heating element and applied zirconia paste used for support of the FeCo MALCs wrapped with a protective, oxide free copper shield. The magnetization was recorded as gradually increasing overall with increasing steps around 500, 600, 875 and 975 K. These can be explained by a transition from hcp Co/α^1 to the higher moment fcc Co (αCo)/α^1 at 500 K and to the higher moment (B2 ordered structure) α^1 at 600K for Co rich segments ($Fe_{32}Co_{68}$). The decrease in M slope at around 800 K may be attributed to the FeO formation as confirmed by HTXRD in Fig. 6 and the annealed MALC microwires in Fig. 5. The small step at 875 K is due to the initial transition into the α (A2) disordered structure of the $Fe_{32}Co_{68}$ regions while the $Fe_{60}Co_{40}$ undergoes a single phase transition from α^1 to α at around 975 K based on recent updates to the Co-Fe phase diagram.[18]

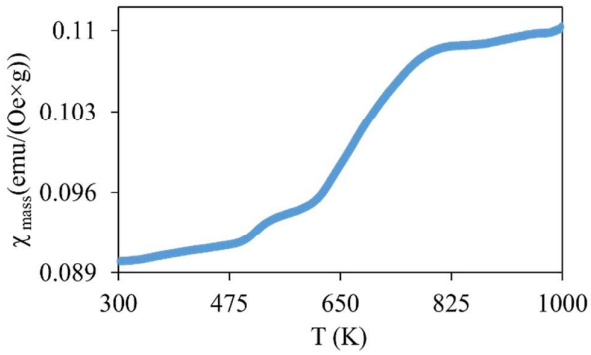

Fig. 9. Mass susceptibility versus temperature (K) from 300 to 1000 K of the FeCo MALCs. Multiple phase transitions are indicated with no decrease in magnetization up to 1000K.

It is apparent from the curve that the magnetization does not decrease (no observable knee) at temperatures up to 1000 K suggesting the absence of single phase bcc Fe (Curie Point ≈ 1043 K) where a transition from a ferromagnetic to paramagnetic state would be expected. [19] While fcc Co possesses T_c (1388 K) higher than that of the FeCo alloy, the presence of pure fcc Co is unlikely due to the high M_s (204 emu/g) reported for the MALCs where the theoretical maximum M_s for bulk fcc Co is < 160 emu/g. The M(T) curve from Fig. 9 therefore substantiates the presence of FeCo alloy present in the sample as T_c for bcc FeCo has been reported at around 1250 K depending on the atomic ratio of Fe and Co respectively. [20]

Discussion

FeCo alloy MALCs were synthesized using the polyol process where a crucial component in the reaction setup for FeCo

MALC formation is the dynamic applied magnetic field driven by a pneumatic piston which oscillates a permanent magnet externally to the sealed reaction vessel. Interestingly, when the applied field was removed, particle morphologies were only present (see supplemental S1). It is well known that external magnetic fields have been used in synthesizing FeCo alloy submicron structures such as thin films by electrodeposition where it was found that the applied field, when parallel to an electrode surface, enhanced FeCo growth rate based on the magnetohydrodynamic effect.[21]

The bcc FeCo alloy was confirmed by XRD and SAED. In addition, two specific diffracting orientations of the FeCo MALCs were analyzed by XRD indicating an isotropic structure. While average chain diameter was found to be approximately 206 ± 52 nm, Scherrer analysis from the most intense (110) plane from XRD analysis gave a crystallite size at ≈ 29 nm indicating that the FeCo segments are polycrystalline. Polished cross-sections by focused ion beam (FIB) on the FeCo MALCs aided in observing the chemical attachment and bonding nature of the FeCo alloy segments. This observation along with TEM imaging indicates well-defined boundaries between FeCo segments following a non-classical growth mechanism whereby carbon coated FeCo crystallites assemble into MALC structures followed by Ostwald ripening and interfacial growth between particles. As previously mentioned, wet chemical synthetic routes, such as the polyol process use glycols as solvents which promote carbon layer formation on particle surfaces due to their relatively high boiling points. While one particular reaction mechanism of the polyol process has been proposed in literature, a confirmed mechanistic route has yet to be accepted. The FeCo MALCs synthesized in this work start with nucleation of Fe^0 and Co^0 on undissolved sodium hydroxide followed by magnetic alignment of FeCo alloy segments onto the permanent magnet surface and continued growth into linear chains.[22] Future work will involve producing FeCo MALCs of smaller diameters well into the nanoscale range with further study on their magnetic properties. Reduction in precursor concentration could prove to be helpful in limiting particle/segment diameters by simply suppressing growth, thus particle size. Presenting a greater challenge, is controlling the aspect ratio of the MALCs. Accurate measurement of the applied external magnetic field strength is required in assessing MALC growth characteristics.

.

Conclusions

FeCo alloys possess several useful properties such as high permeability, high saturation, high Curie temperatures and low coercivity which has been demonstrated by magnetic characterization of the as-synthesized FeCo alloy MALCs produced in this work. FeCo alloy MALCs of 58:42 atomic ratio were created using the polyol process under a specific reaction format whereby FeCo MALC formation was promoted only by a dynamic applied magnetic field. This can be explained by the high permeability to a magnetic field of the FeCo particles, in which, spontaneous alignment of the particles can occur followed by continued growth into MALC structures. This synthesis follows a non-classical growth mechanism. In addition, this synthesis is expected to be highly reproducible in ordinary glassware as long as the same fundamentals provided herein are applied. The as-synthesized FeCo alloy submicron structures as highly magnetic, air stable and non-tethered MALCs are candidates for radar absorbent materials (RAMs) when magnetically oriented in coatings as well as magnetic sensors.

Acknowledgements

D.M.C, C.C., A.J.L. and E.E.C. would like to acknowledge the help of the Virginia Commonwealth University Nanomaterials Characterization Center (NCC).

References

1 Qin, D. H.; Cao, L.; Sun, Q. Y.; Huang, Y.; Li, H. L., Fine magnetic properties obtained in FeCo alloy nanowire arrays. *Chemical Physics Letters* **2002,** *358*, 484-488.
2 Bozorth, R., *Ferromagnetism*. Van Nostrand Company INC.: New York, 1951.
3 Jun, Y. W.; Lee, J. H.; Cheon, J., Chemical design of nanoparticle probes for high-performance magnetic resonance imaging. *Angewandte Chemie* **2008,** *47* (28), 5122-35.
4 López-Ruiz, R.; Magén, C.; Luis, F.; Bartolomé, J., High temperature finite-size effects in the magnetic properties of Ni nanowires. *J. Appl. Phys.* **2012,** *112* (7), 073906.
5 Ramazani, A.; Almasi Kashi, M.; Montazer, A. H., Fabrication of single crystalline, uniaxial single domain Co nanowire arrays with high coercivity. *J. Appl. Phys.* **2014,** *115* (11), 113902.
6 Elıas, A. L.; Rodriguez-Manzo, J. A.; McCartney, M. R.; Golberg, D.; Zamudio, A.; Baltazar, S. E.; Lopez-Urias, F.; Munoz-Sandoval, E.; Gu, L.; Tang, C. C.; Smith, D. J.; Bando, Y.; Terrones, H.; Terrones, M., Production and Characterization of Single-Crystal FeCo Nanowires Inside Carbon Nanotubes. *Nanoletters* **2005,** *5* (3).
7 G. H. Lee, S. H. H., J. W. Jeong, S. H. Kim, and B. J. Choi, CoCr Binary Nanocluster Wires: Enhanced Magnetic Properties of the Co-rich Phase. *Chem. Mater* **2003,** *15*, 504-508.
8 Karipoth, P.; Thirumurugan, A.; Joseyphus, R. J., Synthesis and magnetic properties of flower-like FeCo particles through a one pot polyol process. *J. Colloid Interface Sci.* **2013,** *404*, 49-55.
9 Abbas, M.; Islam, M. N.; Rao, B. P.; Ogawa, T.; Takahashi, M.; Kim, C., One-pot synthesis of high magnetization air-stable FeCo nanoparticles by modified polyol method. *Mater. Lett.* **2013,** *91*, 326-329.
10 Zehani, K.; Bez, R.; Moscovici, J.; Mazaleyrat, F.; Mliki, N.; Bessais, L., High Magnetic Moment of FeCo Nanoparticles Produced in Polyol Medium. *IEEE Trans. Magn.* **2014,** *50* (4), 5.

11 Shokuhfar, A.; Afghahi, S. S. S., Size Controlled Synthesis of FeCo Alloy Nanoparticles and Study of the Particle Size and Distribution Effects on Magnetic Properties. *Adv. Mater. Sci. Eng.* **2014**, 10.
12 Kodama, D.; Shinoda, K.; Sato, K.; Konno, Y.; Joseyphus, R. J.; Motomiya, K.; Takahashi, H.; Matsumoto, T.; Sato, Y.; Tohji, K.; Jeyadevan, B., Chemical Synthesis of Sub-micrometer- to Nanometer-Sized Magnetic FeCo Dice. *Advanced Materials* **2006,** *18* (23), 3154-3159.
13 Zamanpour, M.; Chen, Y. J.; Hu, B. L.; Carroll, K.; Huba, Z. J.; Carpenter, E. E.; Lewis, L. H.; Harris, V. G., Large-scale synthesis of high moment FeCo nanoparticles using modified polyol synthesis. *J. Appl. Phys.* **2012,** *111* (7), 3.
14 Harmen Schippers, T. L., Jaap Heijstek, Modelling of Magnetic Radar Absorbing Composites. In *International Symposium on Electromagnetic Theory*, 2010.
15 Huba, Z. J.; Carroll, K. J.; Carpenter, E. E., Synthesis of high magnetization FeCo alloys prepared by a modified polyol process. *J. Appl. Phys.* **2011,** *109* (7), 3.
16 MacLaren, J. M., Electronic structure, exchange interactions, and Curie temperature of FeCo. *J. Appl. Phys.* **1999,** *85* (8).
17 Clifford, D. M.; El-Gendy, A. A.; Lu, A. J.; Pestov, D.; Carpenter, E. E., Room Temperature Synthesis of Highly Magnetic Cobalt Nanoparticles by Continuous Flow in a Microfluidic Reactor. *Journal of Flow Chemistry* **2014,** *4* (3), 148-152.
18 Okamoto, H., Co-Fe (Cobalt-Iron). *Journal of Phase Equilibria and Diffusion* **2008,** *29* (4), 383-384.
19 H. Stuart, N. R., Lattice parameters and Curie-point anomalies of iron-cobalt alloys. *BRIT. J. APPL. PHYS.* **1969,** *2*.
20 Jacobs, I. S.; Patchen, H. J.; Johnson, N. A., Raising the Curie point in the iron-cobalt-(aluminum) system. *J. Appl. Phys.* **1991,** *69* (8), 5924.
21 Koza, J. A.; Uhlemann, M.; Gebert, A.; Schultz, L., The effect of magnetic fields on the electrodeposition of CoFe alloys. *Electrochimica Acta* **2008,** *53* (16), 5344-5353.
22 Carroll, K. J.; Reveles, J. U.; Shultz, M. D.; Khanna, S. N.; Carpenter, E. E., Preparation of Elemental Cu and Ni Nanoparticles by the Polyol Method: An Experimental and Theoretical Approach. *The Journal of Physical Chemistry C* **2011,** *115* (6), 2656-2664.

FeCo magnetically aligned linear chains (MALCs) were synthesized using polyol based co-precipitation chemistry under an external dynamic magnetic field. These stable, high aspect ratio soft ferromagnetic structures possess values of Ms greater than 200 (emu/g) and Hc (Oe) values less than 200 Oe. They are potential candidates for magnetic switching devices and radar absorbing materials (RAMs) as they can act as nanoscale antenna absorbing radiowaves thru heat conversion when magnetically oriented onto vehicle surface coatings.